Supporting Information

Chuang and Lin 10.1073/pnas.0902675106

SI Materials and Methods

Culture of Primary Sensory Neurons. Newborn rats (postnatal days 0–1, *Rattus norvegicus*) were euthanized by acute decapitation following guidelines of Institutional Animal Care and Use Committee of Cornell University. Dorsal root ganglia and trigeminal ganglia were dissected out, rinsed with Hank's buffer and digested in the same solution containing 1 U/mL type 1 collagenease (Worthington Biochemical Corporation) for 15–30 min at 37 °C. Partially digested tissues were triturated with plastic pipet tips to release neurons into the suspension. The debris was discarded. Neurons in the suspension were centrifuged at 1,000 rpm for 3–5 min. Pellets containing neurons and fibroblasts were re-suspended in 0.25% trypsin and digested for additional 5 min at 37 °C. Cells were spun down, aliquotted onto coverslips coated with polyD-lysine (1 mg/mL) and cultured in Neurobasal Media supplemented with Vitamins and Glutamax (Invitrogen) in an incubator (5% CO_2, 37 °C). Recordings from neuronal membranes were performed within 24 h of culture.

Molecular Biology. cDNAs encoding human, rat, or chicken TRPV1 were subcloned into plasmid vectors designated for expression in both mammalian cells and *Xenopus* oocytes. The 5′ and 3′ regions flanking the ORFs contain the *Xenopus* β-globin untranslated sequences. Point mutations were created by the oligonucleotide-based mutagenesis method, using PCR with Pfu polymerase following the instruction manual of QuikChange site-directed mutagenesis kit (Stratagene). Chimeric receptors were generated by overlapped extension polymerase chain reactions using either Pfu or Phusion (New England Biolabs) polymerase. Capped cRNAs were synthesized by in vitro transcription using linearized plasmid templates and a T7 mMessage Machine kit (Ambion Inc.).

Ratiometric Ca^{2+} Imaging. Cells were loaded with 5 μM fura-2 AM (prepared from a 1 mM concentrated stock dissolved in DMSO) for 2 h in the imagining solution, which contained (in mM) 8.5 HEPES, 140 NaCl, 3.4 KCl, 1.7 $MgCl_2$, and 1 $CaCl_2$, pH 7.4. Solutions in the imaging chambers were gently replaced with the same solutions without dyes. Reactive chemicals or ligands were added to the imaging chambers under stop-flow conditions. Ratios of background-subtracted, emitted fluorescence at excitation wavelengths 340 and 380 nm were displayed in time-lapsed charts. All data were presented as mean ± SEM. from a population of cells.

Electrophysiology. All experiments were conducted at room temperature (22 °C). For oocyte recording, the standard extracellular solution contained (in mM) 5 HEPES, 96 NaCl, 1 $MgCl_2$, and 1 $BaCl_2$, titrated to pH 7.4. The acidic solution was composed of the same ions except with 5 PIPES to replace HEPES, and titrated to pH 6.4 with NaOH.

For mammalian cell recording, the standard extracellular solution had (in mM) 10 HEPES, 145 NaCl or CsCl, 1 $MgCl_2$, and 1 $CaCl_2$, pH 7.4; the standard internal solution contained 10 HEPES, 145 Na gluconate (or 140 Na gluconate plus 6 NaCl for whole cell recordings), 1 $Mg(gluconate)_2$, and 0.1 EGTA, pH 7.4. They were used in the recordings of basal currents (at pH 7.4 in CsCl-based external solution) and ligand-induced currents (in NaCl-based external solution), including capsaicin and 2-APB. For measurement of acid-activated currents in the inside-out configuration, the external solution contained 10 mM PIPES instead of HEPES and 140 mM NaCl to make the final Na^+ concentration 150 mM after titrating with NaOH to final pH 6.4.

For inside-out patch recording, we used patch electrodes pulled from borosilicate capillaries and fire-polished to final diameters (3–10 μm). Giga-ohm membrane seals at cell-attached configuration were formed by gentle suction. Patches were excised into the inside-out configuration afterward. The perfusion tube was placed within 100 μm from the excised patch. Chemicals or ligands were applied following gravity flow, by opening valves controlled by a solenoid. For cell-attached recordings, patch sizes were similar to excised inside-out ones. The perfusion tube was, however, placed at a 1–2-mm distance from the cells.

Voltage ramps from −120 mV to +80 mV given at 1 ramp/s stimulation frequency were routine used to record TRPV1 currents from cells or membrane patches. Between two ramp stimuli, membranes were voltage clamped at −60 mV.

Chemicals. Except capsaicin from Pfaltz and Bauer, 6-iodononivamide and allicin from Axxora, chemicals used in this study were purchased from Sigma-Aldrich. DTT (1 M, aqueous), BAL (10 M, undiluted) ,and other chemicals (prepared as concentrated DMSO stocks) were stored at −20 °C. They were added to recording solutions before experiments and used within the same day.

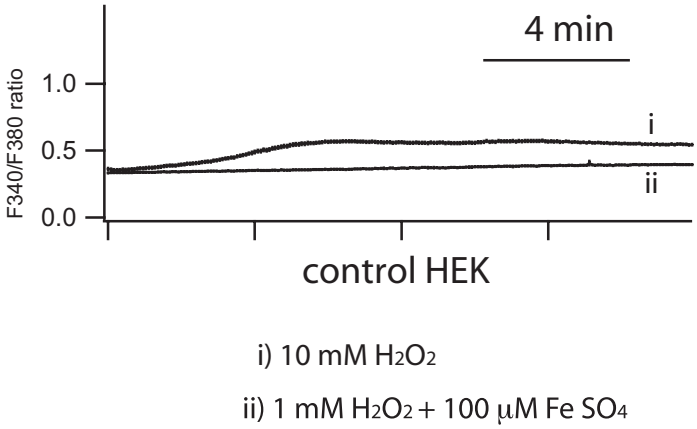

Fig. S1. Ratiometric Ca^{2+} imaging in mock-transfected HEK cells treated with 10 mM H_2O_2 or 1 mM H_2O_2 plus 100 μM iron(II) sulfate showed slight increases of intracellular Ca^{2+} levels above the background but much lower than cells transfected with rat TRPV1 (in Fig. 1*B*).

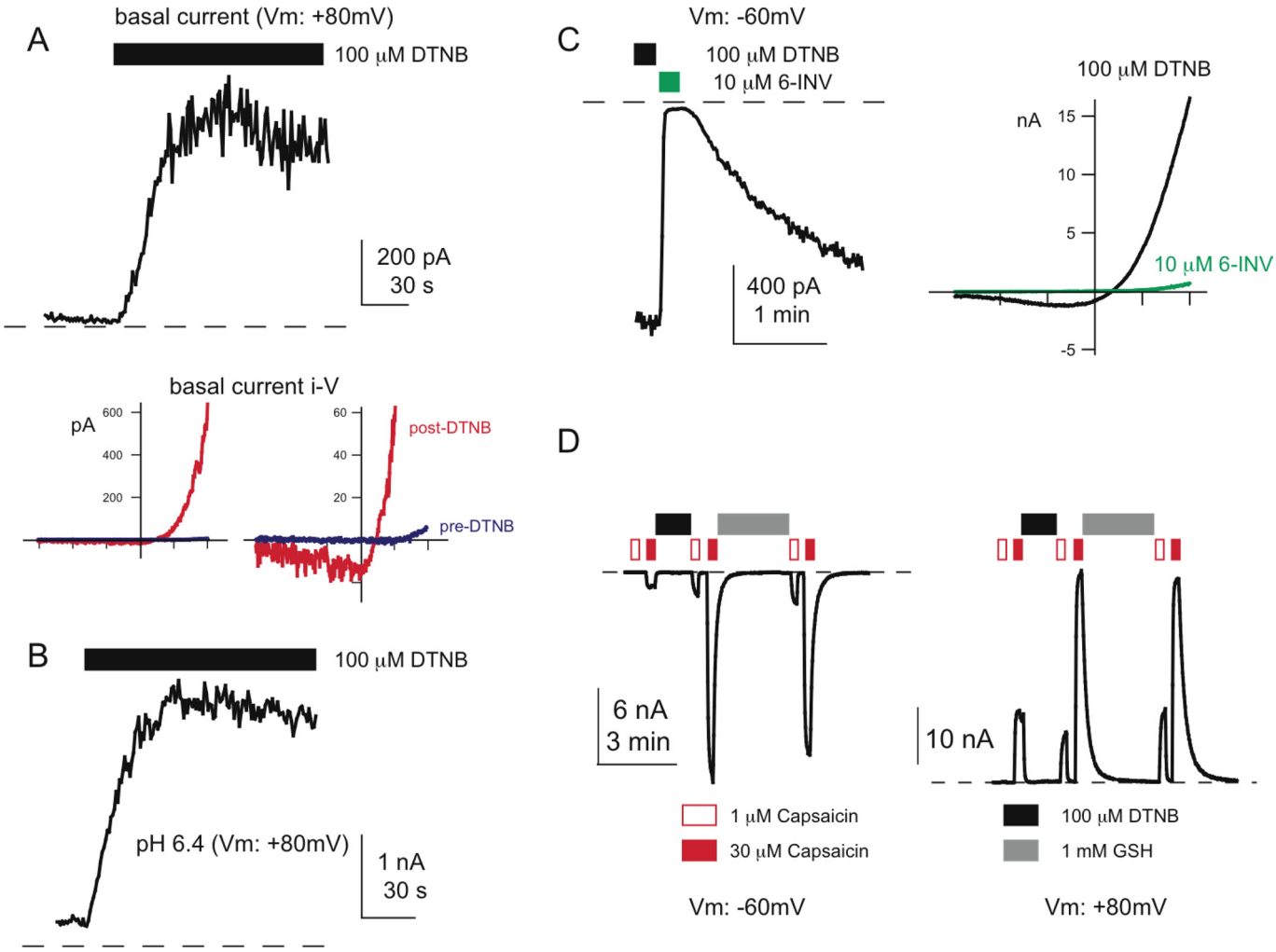

Fig. S2. The oxidizing chemical dithio-bis-nitrobenzoic acid (DTNB) mimics H_2O_2 in sensitizing TRPV1 in inside-out membrane patches with an accelerated kinetics. (*A*) rTRPV1 exhibited minuscule basal activity at very positive membrane voltages. One hundred micromolar DTNB-potentiated rTRPV1 developed discernible inward current at ambient temperature, indicative of the reduction of thermal threshold for receptor activation. Current amplitudes are shown in the upper panel. Ramp traces of the basal currents are shown in the i-V plots of different magnifications. Channel openings are only noticeable at membrane voltages higher than +40 mV before DTNB challenge (blue trace). Discernible inward currents develop after DTNB stimulation (red trace). (*B*) The rTRPV1 current under acidic extracellular pH was also markedly augmented by oxidation. (*C*) DTNB-potentiated rat TRPV1 displayed characteristic outward rectification and selective inhibition by a specific antagonist (6-iodononivamide, 6-INV), confirming the identity of our recorded currents. 6-INV antagonism is more efficient in the negative voltage ranges than in the positive ones. (*D*) DTNB also potentiated the capsaicin-evoked rTRPV1 currents. The potentiation is observed at both 1 μM and 30 μM of capsaicin, and −60 mV or +80 mV alike. It is relatively stable; 3-min application of 1 mM GSH, a weak reducing agent compared to DTT, cannot reverse the potentiation.

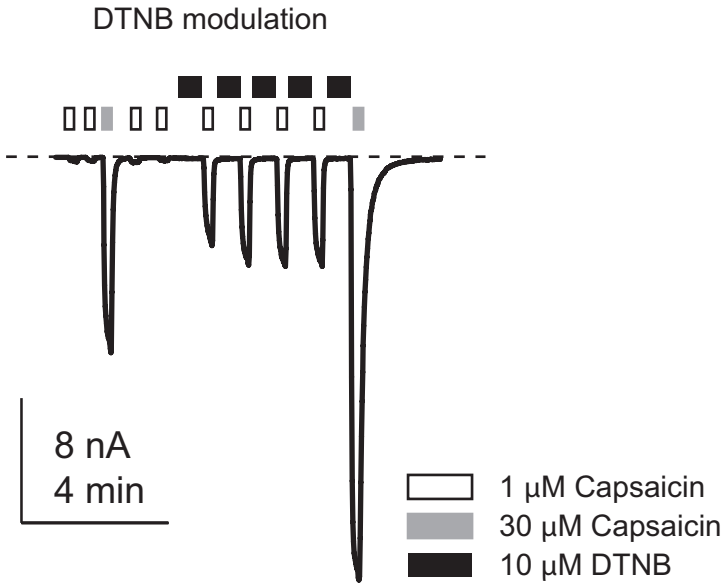

Fig. S3. Sensitization of rat TRPV1 by DTNB displays an increase of receptor currents at both 1 and 30 μM capsaicin. The membrane patch was excised into the inside-out configuration and perfused with bath solutions containing agonists or 10 μM DTNB. At the end of the experiment, 30 μM capsaicin was applied again to evaluate maximal receptor activation. Currents evoked by 1 μM capsaicin after DTNB sensitization approached 30 $\pm$ 13% of currents activated by 30 μM capsaicin ($n = 5$).

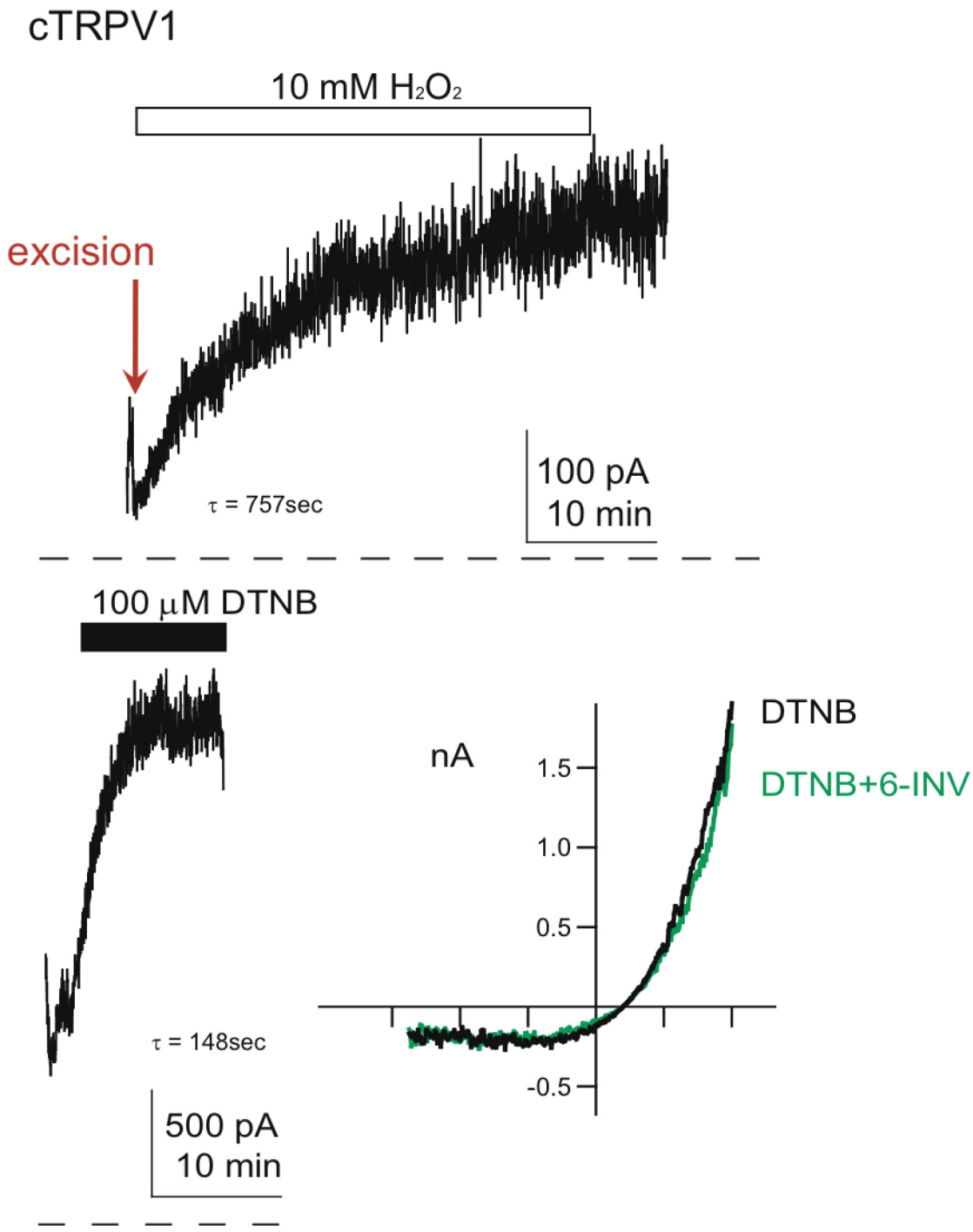

Fig. S4. Chicken TRPV1 is stimulated by 10 mM H_2O_2 with a slow kinetic comparable to the modulation of mammalian TRPV1 (the upper panel, inside-out configuration). Modulation by 100 μM DTNB has a similar feature, but develops much faster (the lower left panel). The DTNB activated basal current of cTRPV1 is, however, refractory to the mammalian TRPV1 antagonist 6-INV (the lower right panel).

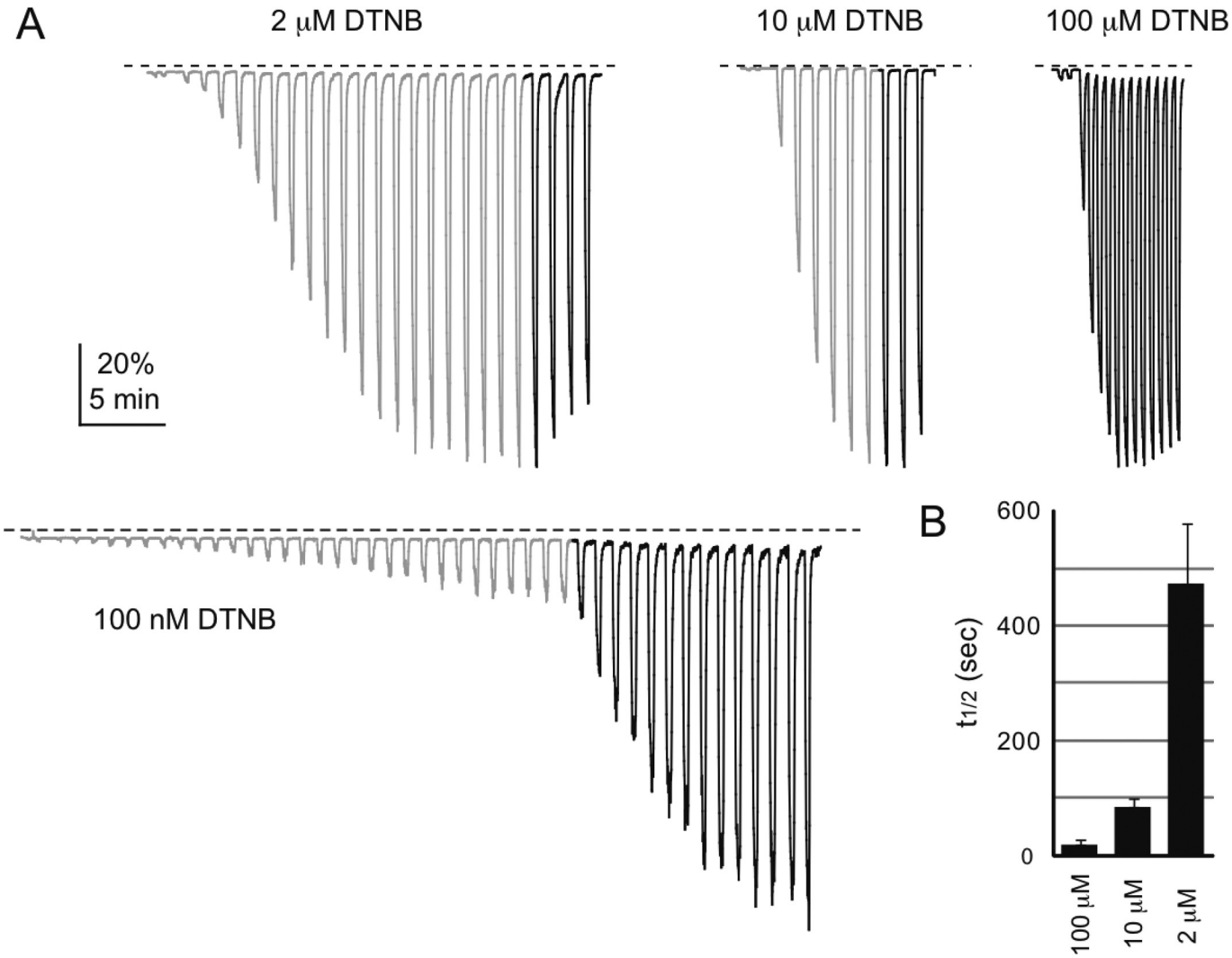

Fig. S5. Rate constants of modulation depend on DTNB concentration, but maximal effects do not. (*A*) Concatenated traces of TRPV1 currents recorded from inside-out patches are displayed in parallel to demonstrate concentration-dependent sensitization kinetics. In all cases, gray and black colors are used to show the effects of two different DTNB concentrations. Typically, 15-s capsaicin pulses (1 μM) are separated by 45-s applications of DTNB. The black-color traces give the maximal potentiation, induced with 100 μM DTNB in the upper panels and with 10 μM DTNB in the lower panel. In the upper rightmost panel, the inter-capsaicin application for 100 μM DTNB is shortened to 15 s to accommodate the fast kinetics. (*B*) The cumulative application time of DTNB for half-maximal stimulation of rTRPV1 is negatively correlated with the concentration of DTNB ($n = 8$ cells for each group). Sensitizations of rTRPV1 after 30-min treatments in 100 nM DTNB (cumulatively 22.5 min) reach 24.6 $\pm$ 5.4% of maximal potentiation ($n = 5$).

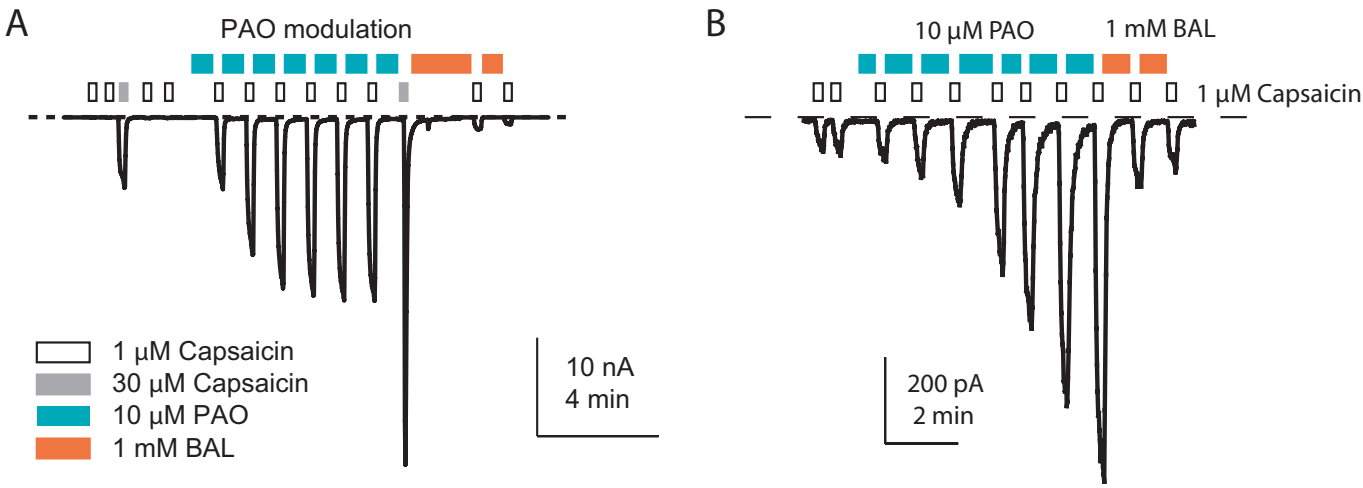

Fig. S6. Sensitization of rat TRPV1 by PAO and its reversal by the dithiol reducing agent BAL. (*A*) The inside-out membrane patch from a HEK cell was perfused with bath solutions containing agonists or 10 μM PAO. 30 μM capsaicin was applied at the end of the experiment to evaluate the maximal level of receptor activation as in Fig. S3. Currents evoked by 1 μM capsaicin after PAO sensitization approached 63 $\pm$ 7% of currents activated by 30 μM capsaicin ($n = 6$). One millimolar BAL application quickly reversed the potentiation. (*B*) Native rat capsaicin receptors are sensitized by PAO. The dithiol reducing agent BAL reverses PAO sensitization. The inside-out membrane patch excised from a cultured primary sensory neuron was perfused with bath solution containing agonists or 10 μM PAO. Currents evoked by 1 μM capsaicin were sensitized by PAO application ($n = 6$). BAL application quickly reversed the potentiation in neuronal membranes as in HEK cell membranes.

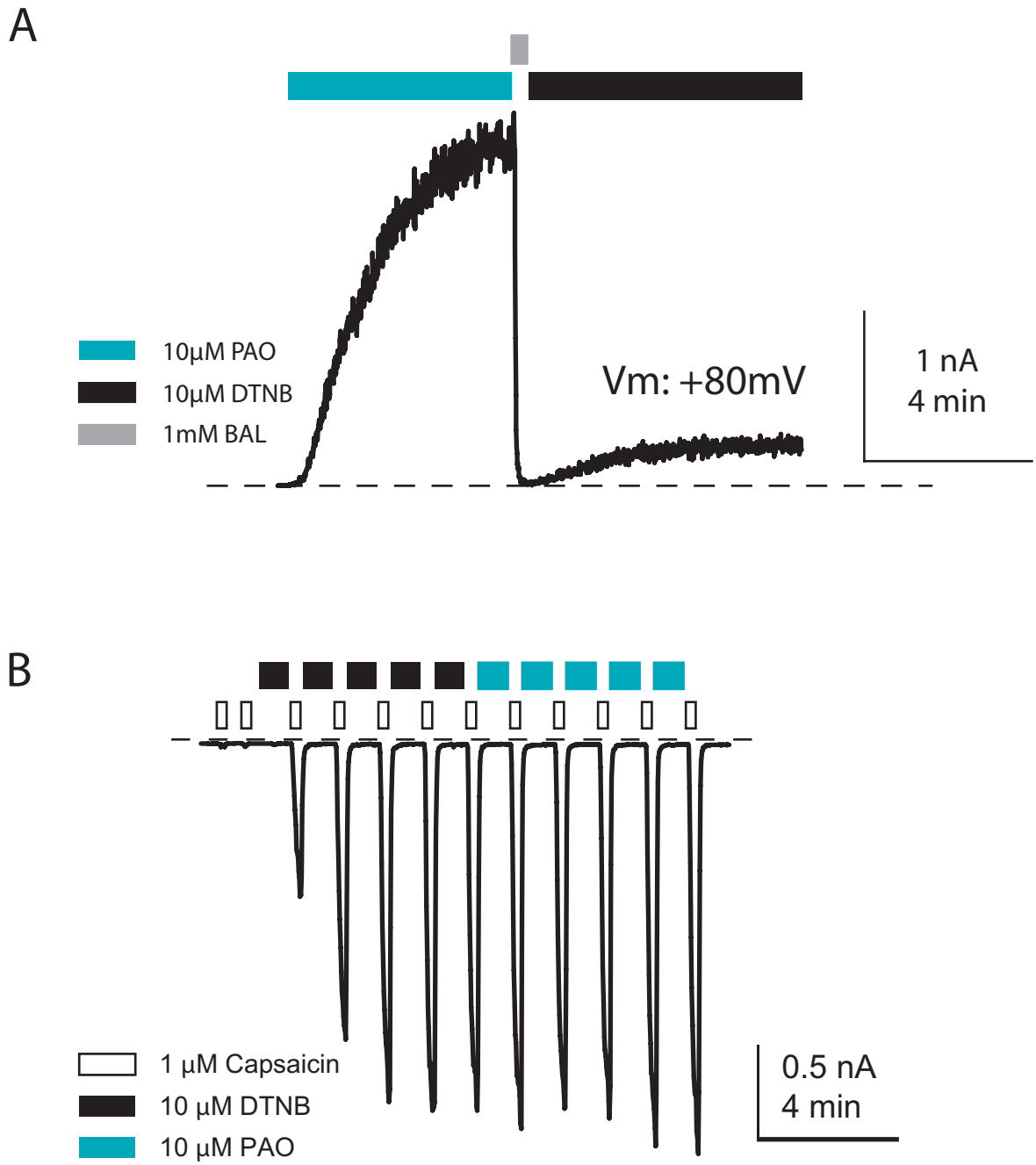

Fig. S7. DTNB modulation and its occlusion of subsequent PAO action. (*A*) Acid (pH 6.4) activated rat TRPV1 was potentiated by either 10 μM PAO or 10 μM DTNB. The inside-out patch was perfused with 1 mM BAL after PAO treatment to recover TRPV1 from sensitization. The following DTNB application stimulated the receptor up to 15 $\pm$ 3% level of the PAO activation ($n = 5$). (*B*) Similar to Fig. 2*B*, DTNB-sensitized rTRPV1 cannot be further potentiated by subsequent application of PAO ($n = 5$).

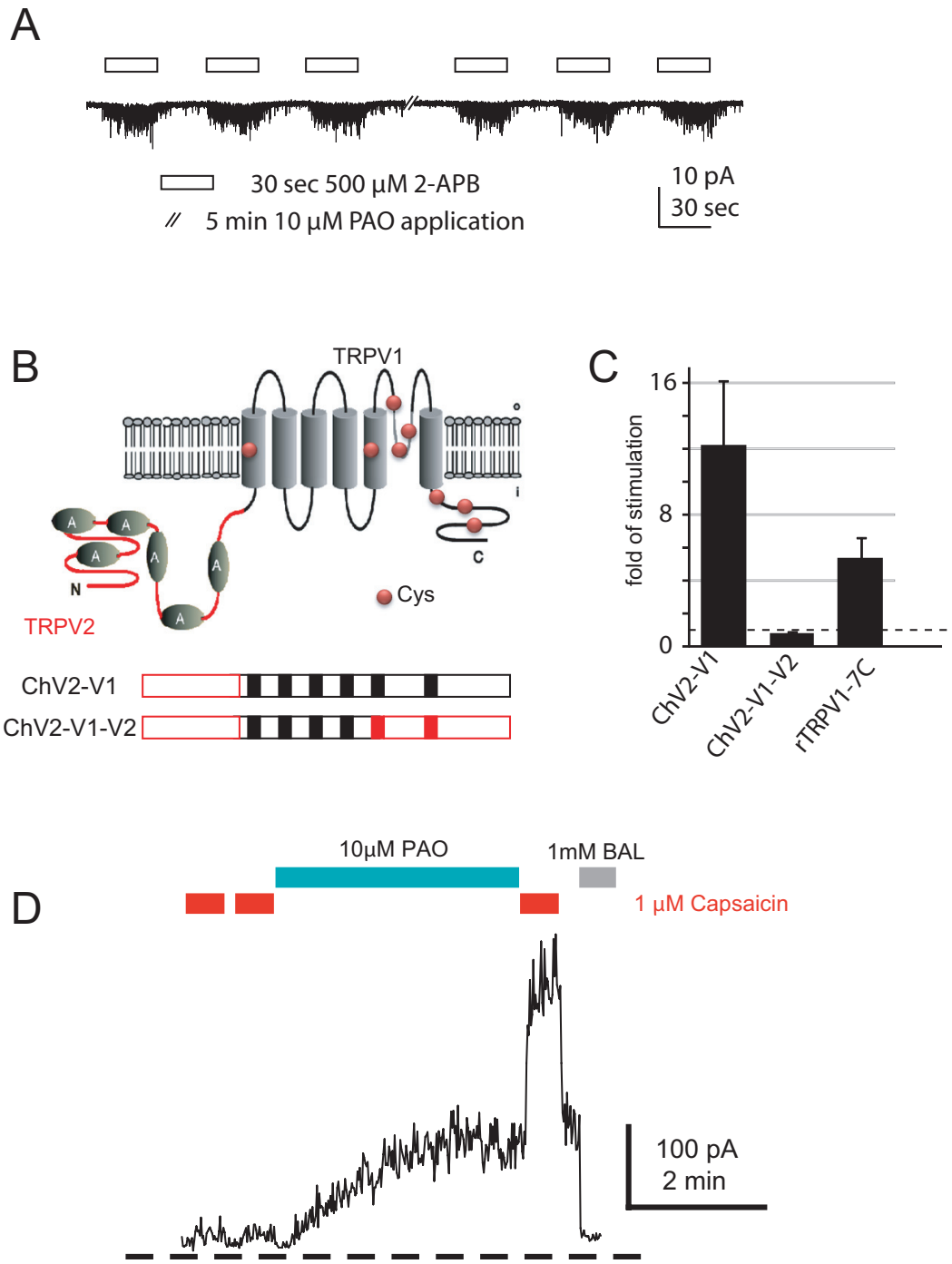

Fig. S8. Oxidative sensitization of TRPV1 requires multiple cysteine residues in the cytoplasmic domains. (*A*) Rat TRPV2 activated by 500 μM 2-APB (2-aminoethoxydiphenyl borate) could not be potentiated by 5 min of 10 μM PAO treatment. The patch was excised from HEK293 cells expressing rat TRPV2 and held at a constant membrane voltage of −60 mV. 2-APB was applied for 30 s for three times each, before and after the PAO treatment. No significant modulation was observed for this channel ($n = 4$). (*B*) Chimera ChV2-V1 (between TRPV1 and TRPV2) transfers the transmembranous and C-terminal domains from TRPV1 to TRPV2, as drawn in the upper panel. Red circle indicates all cysteines residues contained within the TRPV1 fragment in this chimera. The structures of two chimeras, ChV2-V1 and ChV2-V1-V2, are schematized below (TRPV1 in black and TRPV2 in red). Filled boxes represent the transmembrane segments. (*C*) Both N and C termini contain reactive cysteines required for covalent modulation of TRPV1. The dash line in the graph indicates the level of no modulation (fold of stimulation = 1). (*D*) The chicken-rat TRPV1 chimera has the first four transmembrane segments (the capsaicin binding site) transplanted from the rat receptor to the chicken receptor. This chimera responds slightly to capsaicin, but retains the ability to become dramatically sensitized after PAO stimulation. It thus suggests that covalent modification of the cysteines involved in sensitization of wild-type cTRPV1 can successfully couple to ligand (capsaicin) induced channel opening.

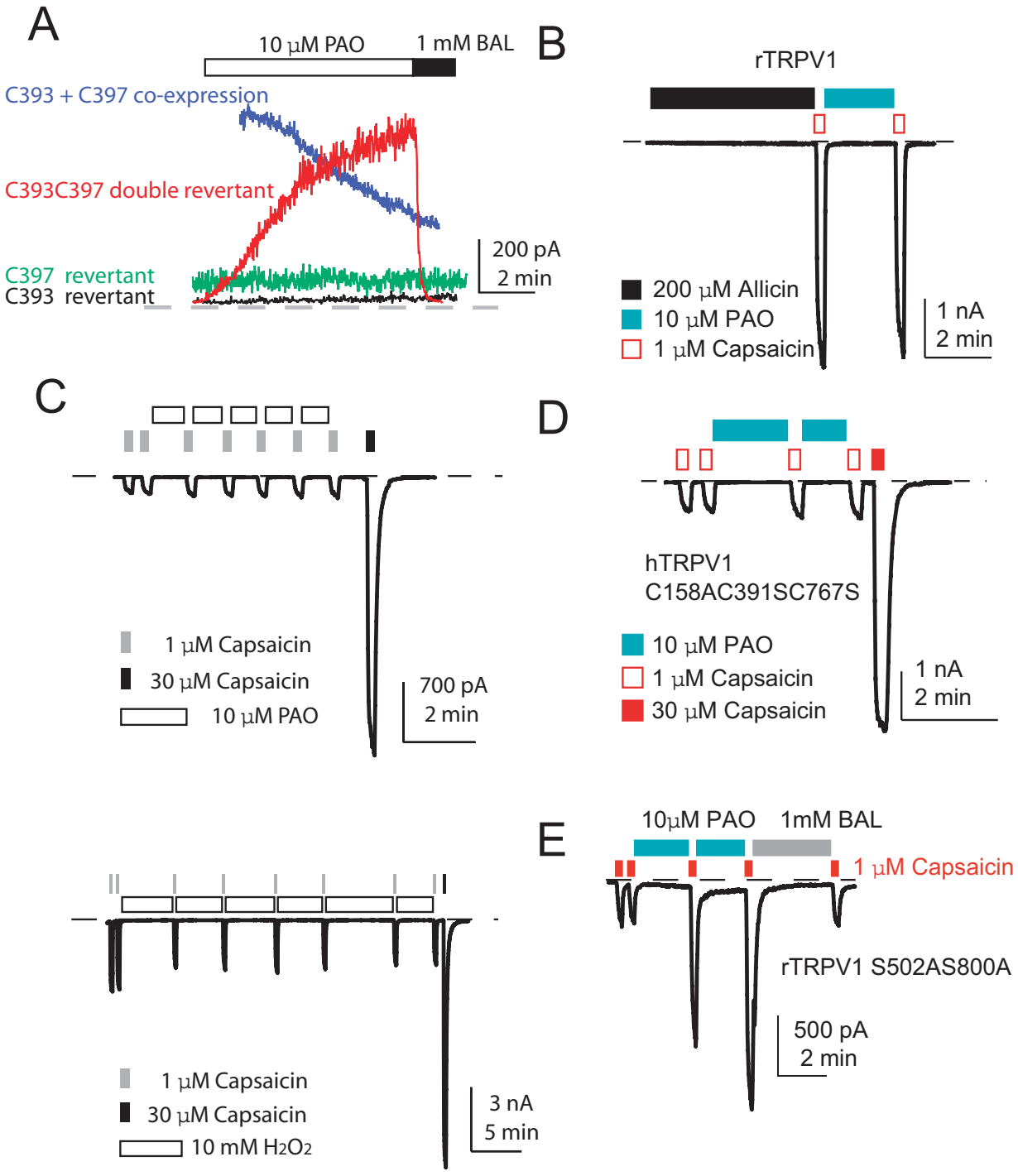

Fig. S9. Mapping modulation-sensitive cysteines. (*A*) Electrophysiological recordings from inside-out patches from HEK cells expressing chicken TRPV1 single revertant C393, C397, the coexpression of the two single revertants, or the double revertant C393C397. Time-lapsed changes of current amplitudes (at + 80 mV of the ramp pulses given at 1 Hz) are shown in different colors. Similar results were observed from 4–5 cells. (*B*) Preapplication of allicin occludes subsequent PAO sensitization of TRPV1. Allicin activated rat TRPV1 is strongly outwardly rectifying with barely noticeable inward currents, but it potentiated receptor activation by 1 μM capsaicin. PAO did not have sensitization effect in cells pretreated with allicin ($n = 4$). (*C*) The quadruple mutation C158AC387SC391SC767S of hTRPV1 is insensitive to either 10 μM PAO (upper panel, $n = 6$) or 10 mM H_2O_2 (lower panel $n = 5$). (*D*) The triple mutation C158AC391SC767S of hTRPV1 cannot form inter-cysteine disulfide bonds required for oxidative sensitization ($n = 5$). The lack of sensitization is not due to maximal agonist occupancy of receptors at 1 μM capsaicin, because 30 μM capsaicin does evoke a much larger current in this mutant. (*E*) The rTRPV1 double mutant (S502AS800A) lacking PKC phosphorylation sites is still sensitized by PAO following the standard protocol for inside-out patch recordings ($n = 5$).

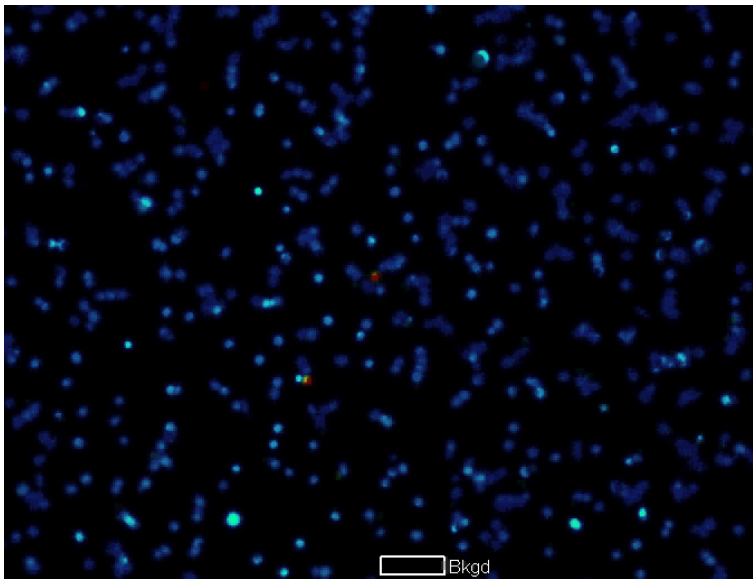

Movie S1. HEK cells expressing rat TRPV1 were loaded with 5 μM Fura-2 AM and imaged at the frame rate of 0.5 Hz for 100 frames. F340/F380 ratios were displayed by pseudocolor codes. 50 μM DTNB was added into the recording chamber. No apparent changes of intracellular Ca^{2+} concentration were noted in the entire population.

Movie S1 (AVI)

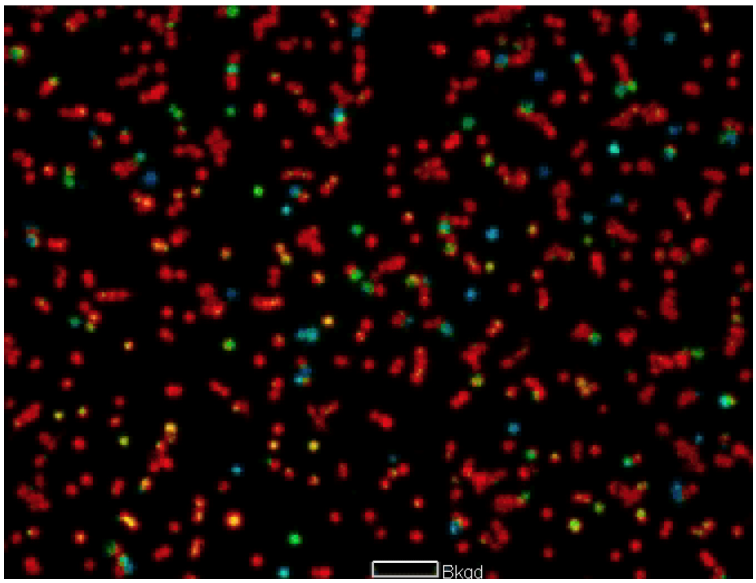

Movie S2. In the same recording chamber, we further added PAO to the final concentration of 13.3 μM. The intracellular Ca^{2+} levels of TRPV1 expressing cells gradually increased, because PAO passed the membrane and activated TRPV1.

Movie S2 (AVI)